

SULFUR DIOXIDE ESTIMATIONS IN THE PLANETARY BOUNDARY LAYER USING OZONE MONITORING INSTRUMENT

J. Zarauz^{a,b}, A. Ghulam^{b,c}, R. Pasken^c

^a Laboratorio Tecnológico del Uruguay (LATU). Av. Italia 6201, Montevideo 11500, Uruguay
jzarauz@latu.org.uy

^b Department of Earth & Atmospheric Sciences, Saint Louis University, MO 63108
rpasken@eas.slu.edu

^c Center for Environmental Sciences, Saint Louis University, MO 63108
jzarauz@slu.edu – ghulam@eas.slu.edu

Commission VI, WG VI/4

KEY WORDS: Sulfur dioxide, OMI, MODIS, Atmospheric pollution

ABSTRACT:

In this paper, we present a method to detect atmospheric pollutants (i.e., SO₂) using Ozone Monitoring Instrument (OMI) and MODerate Resolution Imaging Spectroradiometer (MODIS) data over La Oroya city in Peru. SO₂ loads measured in the planetary boundary layer (PBL) are extracted from the OMI data, and these pollutants are characterized according to their particle size using atmospheric optical depth (AOD) and Ångström coefficient derived from MODIS imagery. The OMI level 2 sulfur dioxide data collected over the test site for the period of 467 days from July 27th, 2007 to November 4th, 2008 are scanned to select candidate datasets that meet the requirements of optimal viewing geometry and cloud conditions. Total of 42 days of satellite measurements that complies with these conditions are used to measure anthropogenic loads, and further validated using field measurements. Results show that there is significant logarithmic correlation between satellite estimated and field measured SO₂, and this correlation can be substantially increased when Ångström exponents are between 0.7 and 1. It is concluded in this contribution that introducing aerosol size distributions may improve SO₂ estimation from satellite data, and there is a greater chance of success for detecting atmospheric pollution when smaller sized aerosols associated with anthropogenic pollutions are dominant.

1. INTRODUCTION

Sulfur dioxide (SO₂) is a gas present in the atmosphere as a result of natural and industrial processes. It is injected into the upper troposphere and lower stratosphere through volcanic activities, and in the Planetary Boundary Layer (PBL) (first 3 km altitude) via anthropogenic emissions contributed by burning fossil fuels (coal and oil), extracting petroleum products, exploiting minerals like aluminium, copper, zinc, iron and lead, and forest fires or agricultural activities.

SO₂ dissolves easily in water and interacts with particles in the air to form sulfates and other products, which may be harmful to the human health. The presence of sulfur dioxide in the PBL affects humans by causing changes in lung function, respiratory disease, irritation of eyes, and cardiac disease, increasing the mortality on days with higher SO₂ levels (WHO 2005). It also affects the environment, contributing to the formation of acid rain and pollution of rivers and lands. Therefore, identifying the potential sources of contamination in the PBL, understanding how SO₂ is spread out over time and space, and quantifying the effects of the gas on public health is of great interest to policy makers, public health advocates and also to general

public. SO₂ can be transported over long distances and deposited far away from the place where it was originally released. New emissions may arise daily, and field measurements are expensive to be performed with reasonable temporal and spatial resolutions. Satellite remote sensing from space provides unique capabilities to measure atmospheric loads of tropospheric chemical constituents.

Satellite based monitoring techniques are coming into widespread use in the estimation of contaminant loads due to its global coverage and improvements in measurement accuracy. Space based monitoring of atmospheric trace gases may be dated back to the launch of NASA's Nimbus-7 spacecraft in 1978 which carried MAPS (Measurement of Air Pollution from Satellites) A – a gas-filter correlation radiometer designed to measure carbon monoxide (CO) and a Total Ozone Mapping Spectrometer (TOMS) aimed at to produce global daily maps of total ozone (O₃), SO₂, H₂SO₄, aerosols in the stratosphere, and UV absorbing aerosols (smoke, dust) over land and oceans. Both instruments were set in orbit onboard of NASA's Nimbus-7 spacecraft and launched on October 24th of that year (BAMS, 2008). The TOMS spectrometer was then onboard of Meteor-3 satellite from August 1991 and TOMS-EP and ADEOS-1 in 1996.

A special joint symposium of ISPRS Technical Commission IV & AutoCarto
in conjunction with
ASPRS/CaGIS 2010 Fall Specialty Conference
November 15-19, 2010 Orlando, Florida

The TOMS instrument measures solar irradiance and radiance backscattered by Earth's atmosphere in six 1 nm wavelength regions at 312, 317, 331, 340, 360, and 380 nm. It uses the ultraviolet part of the electromagnetic spectra, and performs measurements at noon equator crossing time in ascending mode (McPeters et al., 1996). The algorithm used in TOMS SO₂ products is based on differential ozone absorption across a pair of wavelengths. There have been a number of improvements over time on the algorithm. The latest Version 8 takes into account corrections for tropospheric aerosols, brightness from water surfaces, and better temperature and ozone climatology where the latitudinal dependence is minimized (Barthia et al., 2002).

From the launch of GOME sensor aboard of ERS-2 satellite in April 1995 (Burrows et al., 1999) and SCHIAMACHY instrument onboard of ENVISAT spacecraft in March 2002 (Bovensmann et al., 1999), the improvements on spectral resolution has lead to more robust algorithms, i.e., the Differential Optical Absorption Spectroscopy (DOAS) algorithm (Pepijn Veeffkind et al., 2006) to retrieve trace gases. Nevertheless, the temporal resolution of both instruments is very low, 3 and 6 days for GOME and SCHIAMACHY, respectively.

In July, 2004, the Ozone Monitoring Instrument (OMI) was placed in orbit with AURA satellite by NASA and overpasses the equator everyday at 1:45 PM in ascending mode. This sensor has the capability to make a complete scan of the entire Earth in one day, combining the advantages of TOMS, GOME, and SCIAMACHY for a high spatial resolution (13 by 24 km at nadir) and covering the entire UV-VIS spectra (Levelt et al., 2006). OMI uses the Band Residual Difference (BRD) algorithm to retrieve SO₂ at optimum wavelengths significantly improves the measurement accuracy at nadir and middle and low latitudes, by the magnitude of 10 or 20 compared to TOMS algorithm (Krotkov et al., 2006). The great potential of OMI to identify anthropogenic sources like sulfur dioxide have been described by Carn(2007) for smelter and power plants in Peru, Chile, Eastern Europe, Russia, China and Uzbekistan. As it was previously stated, the enhancement on spectral resolution of the latest satellite spectrometers has lead to the detection of heavy anthropogenic loads in the PBL.

The La Oroya smelter, located in central Andes Peru, at 3,700 meters above sea level, is one example of relevant emissions delivered to the atmosphere that could be monitored from the space, and it was the emission source employed on this study.

The company is placed in La Oroya city, 80 km east-northeast from the capital city Lima. The complex topography and daily temperature inversions produced by radiation play an important role on pollutant dispersion through the atmosphere, where the pollution emitted by the smelter remains trapped in the lower troposphere, covering

the city and remaining for long periods of time instead of being dispersed beyond the mountains.

Emissions at this particular site are originated from the stacks and fugitive sources like open buildings, building vents and transport (Integral Consulting Inc, 2005), exceeding on many times the World Health Organization Guidelines (WHO, 2005) shown in Table 1, for each of the pollutants released to the atmosphere (Cedersta, 2002; Klepel, 2005).

	Annual	24 hours	10 minutes
SO ₂		20	500
PM ₁₀	20	50	500
PM _{2.5}	10	25	
TSP	60-90	150-230	
Arsenic			
Lead	0.5		
Cadmium	5 x 10 ⁻³		

Table 1. World Health Organization guidelines. Units are given in µgm⁻³.

Although it is possible to detect heavy anthropogenic loads in the planetary boundary layer (PBL), there have been a few reports in literature dedicated to validate estimations from satellite data and field measurements. The main objectives of this paper are to detect atmospheric pollutants from satellite measurements in Peru, and validate the current BRD algorithm that is used to retrieve SO₂ from the PBL, and further explore the ways to improve measurement performance categorizing the aerosol particle size using atmospheric optical depth (AOD) and the Ångström exponent.

2. STUDY AREA AND DATA

La Oroya smelter in Peru covered 120 km × 120 km with the center coordinates of (11.62S, 75.62W) was selected as the test site. The topography of the area is very complex. The highest elevations extend from northwest to southeast with tops that reach to 5,534 meters, and a maximum slope of 60.5 degrees. On the contrary, the lowest terrain is located northeast at 1,100 meters.

One hour average of SO₂ measurements were obtained on the field from Thermo analyzers, model 43i using the pulsed UV fluorescence method. One of them was placed fix in La Oroya city, 750 m NW from the chimney while the second one was periodically deployed in different locations including Junín (42 km NNW), Huancayo (96 km SE), Concepción (73 km SE) and Jauja (53 km ESE). The main stack located at 11.53S – 75.90W, as well as the sample sites, were within the area of study (Figure 1). The monitoring was carried out from July 27th, 2007 to November 4th, 2008.

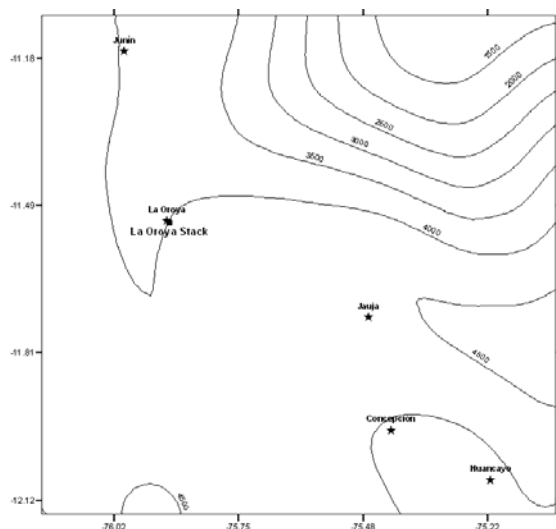


Figure 1. Study area of 120 by 120 km and terrain elevation contours in meters at 500 m interval. Stars indicate the sample sites, while the square shows the main emission source at La Oroya smelter.

With respect to the SO₂ estimations from satellite, OMI level 2, version 3 available online at NASA's Goddard Earth Sciences Data and Information Services Center were used for this study. Since the noise standard deviation of OMI measurements is between 1.2 and 1.5 Dobson Units (DU) in low latitudes, and higher as moving to the poles, only the heavy anthropogenic sources of SO₂ can be detected (Carn et al., 2007; Krotkov et al., 2008).

It is worth to note that the SO₂ measurement sensitivity of OMI in the PBL is limited by sensor viewing geometry and atmospheric conditions, it is necessary to consider only data taken under optimal viewing conditions and free of clouds as shown in Table 2 (OMI Team, 2009). Furthermore, row anomalies for certain days over some cross track positions have been detected by the OMI group (Table 3), and it is not recommended to use them until an effective solution is found to the problem that is currently under investigation. The anomaly number 2 is the one that affected the data set considered in this paper for the days of June 4th, 20th, July 6th, 22nd, 2008.

Optimal viewing conditions	
Cloud fraction	Less than 0.2
Solar zenith angle	Less than 50°
Near nadir viewing angles	Cross track position 10 to 50

Table 2. Optimal viewing conditions recommended by OMI Team, 2009 in order to obtain reliable SO₂ estimations from AURA OMI spectrometer.

Finally, the AOD at 550nm and the Ångström coefficients (based on 470 and 660 nm) were extracted from the Moderate Resolution Imaging Spectroradiometer (MODIS) onboard of satellites Terra (equator crossing time 10:30 AM, descending node) and Aqua (equator crossing time

1:30 PM, ascending node). Both are final products available online at Giovanni data system from NASA GES DISC.

OMI anomaly	From date	Cross track positions
1	June 25 th , 2007	53 – 54
2	May 11 th , 2008	37 – 44
3	January 24 th , 2009	27 – 44

Table 3. Row anomalies detected in the spectrometer and recommended by the OMI group to not be used.

3. METHODOLOGY

3.1 Processing Satellite Data

The hourly SO₂ concentrations for each of the sample sites were analyzed. In order to compare these data with satellite estimations, the average of 1 PM and 2 PM field measurements were computed.

Then, OMI level 2 sulfur dioxide data for the 467 days from July 27th, 2007 to November 4th, 2008 over the study site were extracted by using Longitude, Latitude, Viewing Zenith Angle, Solar Zenith Angle, Reflectivity, Radiative Cloud Fraction, Column Amount SO₂ for the PBL using BRD algorithm, Quality Flags_PBL, Ground Pixel Quality Flags, and Algorithm Flag_PBL from HDF OMI files, and taking only those pixels which corresponds to the location of the surface sample sites. Total 12,788 pixels from AURA OMI data corresponding to the field monitoring sites were selected. Further screening was carried out for optimal viewing conditions that meet the requirements shown in Table 2.

Additional, four more days of observations affected by row anomalies on cross tracks 37 to 44 after May 11th, 2008 were also excluded. Consequently, 46 images met abovementioned predefined conditions were selected for next step analysis.

Due to OMI SO₂ data are expressed in DU (2.69 x 10¹⁶ molecules cm⁻²), it was necessary to convert area density to volumetric density in order to compare satellite measurements against field measurements. A PBL height average of 2,500 meters was assumed for the whole area of study at the time the satellite was over the region. The resultant 55 pixels, corresponding to OMI's optimal viewing conditions, were correlated and plotted with field measurements.

3.2 Aerosol Optical Depth (AOD) and Ångström Coefficient

The Aerosol optical depth (AOD), also named optical thickness (τ), represents the measure of solar radiation extinction produced by aerosol scattering and absorption. It is assumed to be 0 at the top of the atmosphere and increases downward as it approaches the surface. an AOD

A special joint symposium of ISPRS Technical Commission IV & AutoCarto

in conjunction with
ASPRS/CaGIS 2010 Fall Specialty Conference
November 15-19, 2010 Orlando, Florida

value of 0 or close to 0 means clear atmosphere while AODs near 1 represents opacity and pollution.

On the other hand, the Ångström exponent (α) gives an indication of the aerosol size distribution and can be derived from the spectral dependence of the AOD at 2 different wavelengths, 470 and 660 nm for instance (τ_{470} and τ_{660}), as it is expressed in Equation (1).

$$\alpha(\lambda_{660}, \lambda_{470}) = \frac{-\ln\left(\frac{\tau_{660}}{\tau_{470}}\right)}{\ln\left(\frac{\lambda_{660}}{\lambda_{470}}\right)} \quad (1)$$

According to Sabbah et al.(2001) and Askari et al.(2009), the particle size distribution could be identified and categorized by the AOD at 550 nm and by the Ångström coefficient computed from the AOD at 470 and 660 nm, as shown in Table 4. When there is pollution in the atmosphere ($\tau_{550} \geq 0.06$), high Ångström exponents indicate an elevated number of high small aerosol particles, associated with anthropogenic pollutants like SO₂. Contrarily, low Ångström coefficients reflect the presence of coarse mode aerosols or dust.

AOD	Atmospheric condition	Ångström $\alpha_{660/470}$	Aerosol size
$\tau_{550} < 0.06$	Clean		
$\tau_{550} \geq 0.06$	Not clean	< 0.25	Coarse
	Not clean	> 1.0	Fine
	Not clean	0.25 - 1.0	Mixed

Table 4. Aerosol size characterization according to atmospheric optical depth and Ångström exponent.

The AODs and Ångström coefficients were extracted from MODIS data for the 42 days. Then, the days were classified according to the optical depth. Days with AOD less than zero were considered as clear days, free of pollutants, therefore, not considered. Following Sabbah et al. (2001) and Askari et al., (2009), the following metrics were used to distinguish the days with dominant aerosol size or Ångström exponents (α): days were considered as polluted with abundant coarse particles, mainly dust, if α was less than 0.25; if α was greater than 1, fine particles (submicron sizes) were dominant in the atmosphere; when α was between 0.25 and 1, the mixture of these two particles were dominant. As a result, the correlations between the total PBL SO₂ estimated by OMI and field measurements were explored for the days with AOD ≥ 0.06 and $\alpha \leq 1.0$, and days with AOD ≥ 0.06 and $\alpha > 1.0$.

4. RESULTS

The hourly analysis of field measurements, especially at the sample site closest to the main stack reflected that SO₂ concentrations were not constant during the day. They had an extremely daily maximum value of hundreds and

sometimes thousands of PPb during one or two hours at different times and then they drop drastically to less than 10 PPb.

Results showed that OMI underestimated SO₂ for the areas with very high concentrations as it is shown in Figure 2 for the days labelled as 9, 14, 24, and 49 among the 52 observations used. The correlation coefficient between OMI estimations and field measurements was 0.58 (Table 5). However, for low concentrations, the results were considerably better. Extracting the four aforementioned days with very high loads, the OMI SO₂ mean was 6.2 PPb and the mean measured on the field was 5.6 PPb.

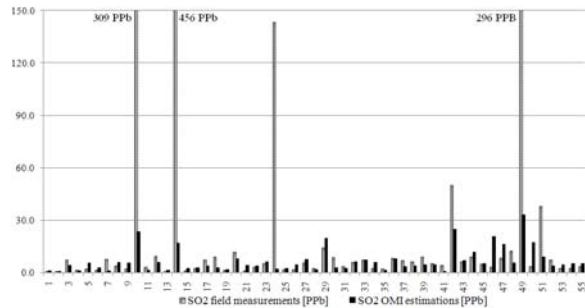


Figure 2. OMI SO₂ PBL retrieved by BRD algorithm (grey) and SO₂ field measurements (black). Units are expressed in PPb.

A logarithmic model was found between field measurements and OMI estimations as shown in Figure 3. This implied that satellite spectrum may saturate when SO₂ loads reached certain concentration level, and that a reliable estimation with acceptable accuracy could be made when anthropogenic pollution was less than this threshold. While the high pollution loads were challenging to accurately measure according to our results, this observation could serve as an early warning for public health issues.

When the sample days were characterized according to the aerosol size distribution, the Ångström exponent laid between 0.7 and 1.0 for coarse particles and 1.0 to 1.8 for fine particles.

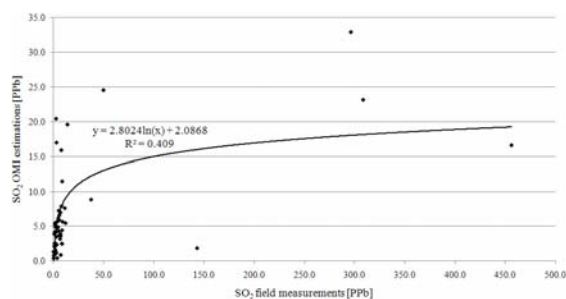


Figure 3. Logarithmic relationship between OMI SO₂ PBL retrieved by BRD algorithm (left) and SO₂ field measurements (bottom). Units are expressed in PPb.

The correlation coefficients between satellite and field data considering only fine particulates was 0.41 (Table 6), and significantly increased up to 0.69 when only the coarse aerosols were taken into account (Table 7).

	SO ₂ field meas.	OMI SO ₂	AOD	Ångström coef.
Correlation	0.58			
Max	456.4	32.9	0.2	1.8
Min	0.2	0.4	0.0	0.7
StDev	83.4	6.8	0.1	0.32
Mean	27.6	6.5	0.1	1.2

Table 5. Statistic information of SO₂ field measurements and SO₂ estimated by OMI. All of the days with optimal viewing conditions are considered. Units are expressed in PPb.

	SO ₂ field meas.	OMI SO ₂	AOD	Ångström coef.
Correlation	0.41			
Max	456.4	19.6	2.4	1.8
Min	0.2	0.2	0.0	0.0
StDev	73.6	4.3	0.4	0.3
Mean	22.3	5.3	0.1	1.3

Table 6. Statistic information of SO₂ field measurements and SO₂ estimated by OMI. Only days with AOD ≥ 0.06 and Ångström coefficient ≥ 1 are considered. Units are expressed in PPb.

Since the detection of SO₂ in the planetary boundary layer (PBL) depends on the reflectivity in the lower troposphere, and because of aerosol effects are not accounted in the BRD algorithm (Carn et al., 2007) used in this study, it was evident from results that aerosol size classification should be incorporated to estimate SO₂ loads.

	SO ₂ field meas.	OMI SO ₂	AOD	Ångström coef.
Correlation	0.69			
Max	308.6	23.2	0.2	1.0
Min	0.5	0.8	0.1	0.7
StDev	101.4	6.6	0.0	0.1
Mean	43.6	6.6	0.1	0.9

Table 7. Statistic information of SO₂ field measurements and SO₂ estimated by OMI. Only days with AOD ≥ 0.06 and Ångström coefficient < 1 are considered. Units are expressed in PPb.

It is worth noting that the coefficient of correlation was increased from 0.58 to 0.69 when only the days with Ångström exponents less than 1 were considered. As a result of existing coarse particles that result in the increment of the extinction coefficient, the Ångström exponent decreases, and therefore, the amount of solar

radiation scattered back from the atmosphere and intercepted by the satellite sensor increases. With respect to total O₃, an increase from 325 DU to 425 DU only decreases the air mass factor in 10% (Krotkov et al., 2008). The correlation difference should not be attributed to this factor because the total O₃ remained almost constant, between 212 to 279 DU for the entire period of time covered by this study.

5. CONCLUSIONS

This paper explored the efficacy of satellite measurements in detecting anthropogenic pollutant loads, and the ways to improve the accuracy of the estimations incorporating the multi-source satellite data including the Ozone Monitoring Instrument (OMI) and the MODerate Resolution Imaging Spectroradiometer (MODIS).

The analysis of hourly based SO₂ field measurements indicated that emission peaks may be difficult to be detected by OMI since the peak hours do not always occur at the same time the satellite make its overpass. The overall correlation coefficient between OMI and field measurements was 0.58. The coefficient of correlation was increased from 0.58 to 0.69 when only the days with Ångström exponents less than 1 were considered. On the contrary, when days with Ångström exponents greater than 1 were considered, the coefficient of correlation between the satellite estimation and field measurements decreased from 0.58 to 0.41. High Ångström coefficients ranges from 1 to 1.8 means that fine particulates with larger SO₂ concentrations are dominant in the atmosphere.

The significant SO₂ loads could result in stronger absorption, and therefore, lower signal-to-noise ratio and/or saturation of measured spectrum due to larger concentrations. This fact could also explain the underestimations of OMI measurements during days of very high SO₂ loads observed on the sample sites.

When the aforementioned SO₂ concentration maximums were excluded from the datasets, the temporal and spatial mean values for OMI and field measurements demonstrated significant agreement of 6.2 over 5.6 PPb.

A logarithmic relationship was detected when field measurements were plotted against the OMI data. This indicated that the space based measurement with significant accuracy may be challenging when anthropogenic pollution loads are dominant in the planetary boundary layer. However, it can be deduced from the results that, we stand a greater chance of success detecting the pollutants when the concentration is lower, which has important public health implications.

This contribution also found that the characterization of aerosol sizes for Ångström exponents were helpful improving estimation accuracy, however, further studies are needed to reach such a conclusion.

6. REFERENCES

- BAMS, 2008. Seeing pollution from space. *Bulletin of the American Meteorological Society*, 89(6), pp. 805-821.
- Barthia, P. and Wellemeyer, W., 2002. "TOMS-V8 total ozone algorithm" in OMI Algorithm Theoretical Basis Document, OMI Ozone Products, P. K. Barthia, Ed. *Greenbelt*, MD: NASA/Goddard Space Flight Center, 2.
- Bovensmann, H., Burrows, J., Buchwitz, M., Frerick, J., Noel, S. and Rozanov, V., 1999. SCIAMACHY: Mission Objectives and Measurement Modes. *Journal of Atmospheric Sciences*, 56(2).
- Burrows J., et al., 1999. The Global Ozone Monitoring Experiment (GOME): Mission Concept and First Scientific Results. *Journal of Applied Sciences*. 56(2), pp.151-175
- Carn, S.A., Krueger, A.J., Krotkov, N.A., Yang, K., Levelt, P.F., 2007. Sulfur dioxide emissions from Peruvian copper smelters detected by the Ozone Monitoring Instrument. *Geophysical Research Letters*, 34, L09801, doi:10.1029/2006GL02902.
- Cedersta A., Barandiarán G., 2002: La Oroya cannot wait. *Interamerican Association for Environmental Defense (AIDA) and Peruvian Society for Environmental Law (SPDA)*, 1st Edition, pp. 123.
- El-Askari, H., R. Farouk, C. Ichoku, and M. Kafatos, 2009. Transport of dust and anthropogenic aerosols across Alexandria, Egypt, *Annales Geophysicae*, 27, 2869-2879.
- Integral Consulting Inc, 2005: Air quality dispersion modeling for human health risk assessment. Prepared by Mc Vehil-Monnet Associates Inc. 44 Inverness Dr. E. Bldg. C, Englewood, CO 80112. MMA project number 1875-0.
- Krotkov, N.A., Carn, S.A., Krueger, A.J., Bharthia, P.K., and Yang, K., 2006. Band residual difference algorithm for retrieval of SO₂ from the AURA Ozone Monitoring Instrument (OMI). *IEEE Transactions on Geoscience and Remote Sensing*, 44(5), pp. 1259 – 1266.
- Krotkov, N.A., B. McClure, R. R. Dickerson, S. Carn, C. Li, P. K. Bharthia, K. Yang, A. Krueger, Z. Li, P. F. Levelt, H. Chen, P. Wang, and D. Lu, 2008. Validation of SO₂ retrievals from the Ozone Monitoring Instrument (OMI) over NE China. *Journal of Geophysical Research*, 13.
- Levelt, P.F., van den Oord, H.J., Dobber M.R., Malkki, A., Visser, H., de Vries, J., Stammes, P., Lundell, J.O.V., and Saari, H., 2006. The Ozone Monitoring Instrument. *IEEE Transactions on Geoscience and remote Sensing*, 44(5), pp. 1093-1101.
- McPeters, R., Bharthia, P., Krueger, A., Herman, J., Schlesinger, B., Wellemeyer, C., Seftor, C., Jaross, G., Taylor, S., Swissler, T., Torres, O., Labow, G., Byerly, W., and Cebula, R., 1996. Nimbus-7 Total Ozone Mapping Spectrometer (TOMS) Data Products User's Guide.
- OMI Team, 2009. Ozone Monitoring Instrument (OMI), data user's guide. http://disc.sci.gsfc.nasa.gov/Aura/data-holdings/additional/documentation/README.OMI_DUG. Df, NASA's Goddard Earth Sciences Data and Information Services Center (accessed 1 Sep. 2010).
- Pepijn Veefkind, J., J.F. de Haan, E.J. Brinksma, M. Kroon, and P.F. Levelt, 2006: Total ozone from the Ozone Monitoring Instrument (OMI) using the DOAS technique. *IEEE Transactions on Geoscience and Remote Sensing*, 44(5).
- Sabbah, I., C. Ichoku, Y.J. Kaufman, and L.A. Remer, 2001. Full year cycle of desert dust spectral optical thickness and precipitable water vapor over Alexandria, Egypt, *Journal of Geophysical Research*, 106, pp.18305-18316.
- WHO, 2005. Air quality guidelines for particulate matter, ozone, nitrogen, dioxide and sulfur dioxide. Global update 2005. WHO/SDE/PHE/OEH/06.02. http://whqlibdoc.who.int/hq/2006/WHO_SDE_PHE_OEH_06.02_eng.pdf (accessed 1 Sep. 2010).

7. ACKNOWLEDGEMENTS

The authors wish to thank the Archbishop of Huancayo Province (Peru) for the provision of sulfur dioxide data.

Analyses and visualizations used in this paper were produced with the Giovanni online data system, developed and maintained by the NASA GES DISC.